Understanding the enhanced electrochemical performance of samarium substituted Li[Li$_{0.2}$Mn$_{0.54-x}$Sm$_x$Co$_{0.13}$Ni$_{0.13}$]O$_2$ cathode material for lithium ion batteries

Guofeng Xu [a], Qingrui Xue [a], Jianling Li [a,*], Zhanyu Li [a], Xinping Li [a], Tianheng Yu [a], Jiguang Li [a], Xindong Wang [a], Feiyu Kang [b]

[a] School of Metallurgical and Ecological Engineering, University of Science and Technology Beijing, Beijing 100083, China
[b] Lab of Advanced Materials, Department of Materials Science and Engineering, Tsinghua University, Beijing 100084, China

ARTICLE INFO

ABSTRACT

Lithium-excess layered cathode materials Li[Li$_{0.2}$Mn$_{0.54-x}$Sm$_x$Co$_{0.13}$Ni$_{0.13}$]O$_2$ (x = 0, 0.01, 0.03, 0.05) with different quantities of Sm were synthesized by the coprecipitation-calcination method. The rare earth element samarium (Sm) was introduced into the structure of Li[Li$_{0.2}$Mn$_{0.54}$Co$_{0.13}$Ni$_{0.13}$]O$_2$ as the replacement at Mn sites. The refinement unit cell parameters from the X-ray powder diffraction patterns illustrate the doping of Sm facilitates enlarging the lithium ions diffusion passageway space of the Li[Li$_{0.2}$Mn$_{0.54}$Co$_{0.13}$Ni$_{0.13}$]O$_2$ structure. The Li[Li$_{0.2}$Mn$_{0.51}$Sm$_{0.03}$Co$_{0.13}$Ni$_{0.13}$]O$_2$ electrode presented the best electrochemistry properties. The initial discharge capacity is 287.5 mAh g^{-1} and the initial coulombic efficiency increases from 81.31% to 85.34% with a constant current density of 12.5 mA g^{-1}, which can be attributed to the suppression of the oxygen release from the structure at the initial charge-discharge process. The Li[Li$_{0.2}$Mn$_{0.51}$Sm$_{0.03}$Co$_{0.13}$Ni$_{0.13}$]O$_2$ electrode delivers 236.1 mAh g^{-1} after 40 cycles and the capacity retention ratio is 82.12% while only 206.8 mAh g^{-1} and 70.85% are obtained after 40 times of cycling for the pristine electrode. The Nyquist plots indicate that the electrical conductivity and interfacial electrochemical reaction activity increase as well.

1. Introduction

The lithium-excess layered cathode materials xLi$_2$MnO$_3$·(1−x)LiMO$_2$ or Li$_{1+x}$M$_{1-x}$O$_2$ (M is a transition metal or a mixture of transition metals) are quite promising due to the reversible capacity of up to 280 mAh g^{-1} and the wide working voltage range and low cost [1–3]. Although extensive researches have been carried out, there are some drawbacks to overcome for the further application of lithium-rich cathode. The large irreversible capacity loss during the initial cycle has a significant impact on the subsequent charge and discharge capacity [4,5]. The mechanisms of lithium transference and structure evolution during the initial and succeeding cycles require further investigation. The cathode exhibits awful rate capability because of the existence of the low electronic conductivity ingredient Li$_2$MnO$_3$. In addition, the cathode also presents a gradual capacity drop by reason of local phase transformation during cycling [6–9].

Substitutions with other elements were adopted to overcome the disadvantages above, with regard to the specific role of transition metal manganese in the lithium-rich cathode materials. Al^{3+}, Mg^{2+}

and Ru^{x+} are generally employed to stabilize the microstructure of the materials, enhance the lithium ion diffusion rate within the materials and suppress the transformation of local structure [10,11]. Besides, anion F$^-$ is usually adopted to substitute the O$_{2p}$ in order to optimize the electrochemical performance on account of the strong F–O chemical bond which could restrain the oxygen evolution from the crystal lattice during the first charge-discharge process [12,13].

In addition to the oxygen evolution issue, the behavior of manganese also has an effect on the local structure transmutation during cycling. Quadrivalent manganese ions in the center of the octahedron occupy the lithium ion vacancies at 3a position after the lithium ions have been extracted. The following intercalation of lithium ions leads to irreversible phase transition from layer structure to spinel-like phase [14, 15]. In this paper, we propose to introduce the rare earth element samarium (Sm) into the lithium-excess layered structure of Li[Li$_{0.2}$Mn$_{0.54}$Co$_{0.13}$Ni$_{0.13}$]O$_2$ as the replacement at Mn sites to explore the possibilities for solving the problems above. On one hand, the large ionic radius of Sm^{3+} and the big binding force of Sm–O make the lattice structure tending towards stability. On the other hand, the good electronic conductivity of cation Sm^{3+} could enhance the charge transference at the time of Li$^+$ extraction and insertion. In this case, the substitution of Sm in place of Mn is expected to restrain the lattice

* Corresponding author.
E-mail address: lijianling@ustb.edu.cn (J. Li).

structure from phase transformation and improve the Li + diffusion efficiency in the meantime. Thereby, the mechanisms of transition metal elements diffusion and local phase transformation are investigated.

In this work, convenient coprecipitation technique is employed to synthesis nanoscale lithium-excess layered oxide. Element Sm is adopted to substitute manganese in the calcining process to prepare $Li[Li_{0.2}Mn_{0.54-x}Sm_xCo_{0.13}Ni_{0.13}]O_2$. Crystal structure, lattice parameters, morphology, electrochemical performances and the charging-discharging mechanism of Sm-substituted cathode are thoroughly studied.

2. Experimental

2.1. Material preparation

Li-excess layered cathode materials $Li[Li_{0.2}Mn_{0.54-x}Sm_xCo_{0.13}Ni_{0.13}]O_2$ with different quantities of doped Sm was synthesized by a coprecipitation-calcination method, in which x equals to 0, 0.01, 0.02 and 0.03. $NiSO_4 \cdot 6H_2O$, $CoSO_4 \cdot 7H_2O$ and $MnSO_4 \cdot H_2O$ (AR, Sinopharm Chemical Reagent Co., Ltd) with cationic mole ratio of Ni:Co:Mn = 0.13:0.13:(0.54−x) were dissolved to form mixed solution A of 2 mol L^{-1}. The precipitant KOH (AR, Sinopharm Chemical Reagent Co., Ltd) and buffering agent NH_4OH (AR, Sinopharm Chemical Reagent Co., Ltd) were mixed to form aqueous solution B of 4 mol L^{-1} with a mole ratio of KOH:NH_4OH = 3:2. The mixed solutions A and B were pumped into a continuously stirred tank reactor which had been filled with argon atmosphere. After being stirred for 5 min with the controlled pH value of 12, the synthesized precursor was filtered and washed with distilled deionized water, and dried in a vacuum oven at 100 °w for 12 h. The dried precursor, stoichiometric $LiOH \cdot H_2O$ (AR, Sinopharm Chemical Reagent Co., Ltd) which was 5 wt.% excess and

Table 1
Refined unit cell parameters, interlayer and layer spaces of the prepared $Li[Li_{0.2}Mn_{0.54-x}Sm_xCo_{0.13}Ni_{0.13}]O_2$ samples.

| x	a (Å)	c (Å)	V (Å³)	c/a	$I_{(003)/(104)}$	S_{TM} (Å)	I_{Li} (Å)
0	2.85494	14.25371	100.6	4.993	1.2047	2.62933	2.12191
0.01	2.85207	14.39860	101.4	5.048	1.2458	2.65606	2.14344
0.03	2.85316	14.39963	101.5	5.047	1.2763	2.65625	2.14363
0.05	2.85382	14.40031	101.6	5.045	1.3128	2.65638	2.14372

stoichiometric Sm_2O_3 (AR, Aladdin Chemistry Co., Ltd) were mixed and thoroughly grinded in a ball mill. The mixture was transferred into the furnace, preheated at 450 °i for 4 h and then calcined at 900 ° for 24 h. And the obtained powders were quenched with liquid nitrogen.

2.2. Structure and morphology characterization

The structures and morphologies of the pristine and Sm-substituted $Li[Li_{0.2}Mn_{0.54-x}Sm_xCo_{0.13}Ni_{0.13}]O_2$ samples were analyzed by powder X-ray diffraction (XRD, Rigaku RINT2400 with Cu Ka radiation, λ = 1.54056 Å, Japan) and field-emission scanning electron microscopy (FESEM, Zeiss SuprATM 55 microscope, German). The relative amounts of Li, Mn, Ni, and Co, Sm in the samples were monitored by conducting inductively coupled plasma-atomic emission spectrometry (ICP-AES, OPTIMA 7000DV, PerkinElmer Co., Ltd., America). Energy-dispersive X-ray spectroscopy (EDS, Kevex SuperDry, America) analyses were conducted to test the elemental distributions on the surface of cathode materials.

2.3. Electrochemical test

Electrochemical performances of the prepared samples were tested by CR2025 coin cells and the work electrodes were fabricated by the draw-off method using aluminium foil as the current collector. Polyvinylidene fluoride (PVDF, Arkema HSV900) was dissolved into the 1-methyl-2-pyrrolidone (AR, Sinopharm Chemical Reagent Co., Ltd) as the binder solution. A mixture of active material and acetylene black was thoroughly milled and homogeneously blended into the binder solution. The weight ratio of active material, acetylene black and PVDF is 75:15:10. The as-prepared slurry was coated and compressed onto the current collector with the coating thickness of 4 mg cm^{-2}, and then dried at 100 ° for 12 h under vacuum. Wafer cathodes with the diameters of 10 mm were punched for use. The assembling of coin cells was conducted in glovebox full filled with high-purify argon gas. The electrolyte was 1 mol L^{-1} $LiPF_6$ in a mixed solvent of ethylenecarbonate (EC) and dimethylcarbonate (DMC) with the volume ratio of 1:1 (purchased from Zhangjiagang Guotai Huarong Chemical New Material Co., Ltd.) and the porous polypropylene film (Celgard 2400) was placed between cathode and anode. The initial galvanostatic charge-discharge test was studied at 12.5 mA g^{-1} and the cycling performance was carried out with 25.0 mA g^{-1} in the voltage range of 2.0–4.8 V. For the rate tests, cells were charged to 4.8 V at 0.1C (25.0 mA g^{-1}) and discharged to 2.0 V at different rates successively. Electrochemical impedance spectroscopy (EIS) was adopted on VMP2 electrochemical workstation (Princeton Applied Research, USA) in the
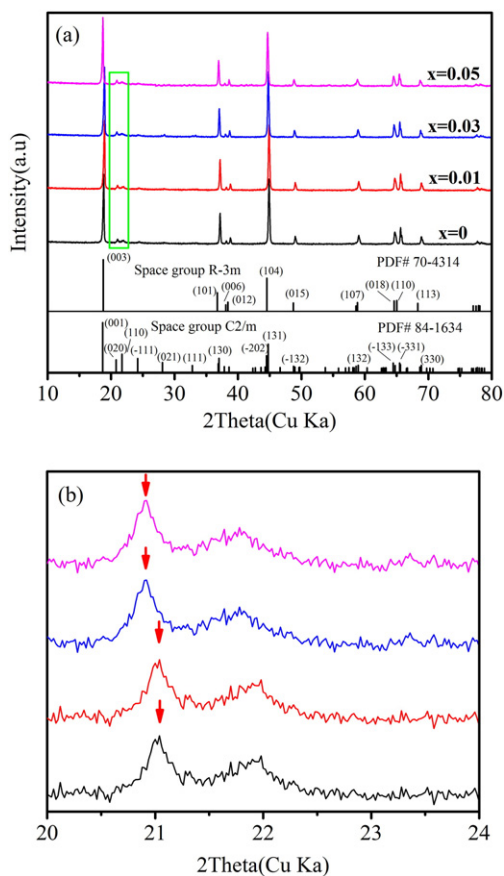
Fig. 1. XRD patterns (a) and the partial enlargement (b) of the prepared $Li[Li_{0.2}Mn_{0.54-x}Sm_xCo_{0.13}Ni_{0.13}]O_2$ samples.

Table 2
Relative contents of Li, Ni, Co, Mn and Sm in the pristine and Sm-doped $Li[Li_{0.2}Mn_{0.54-x}Sm_xCo_{0.13}Ni_{0.13}]O_2$ samples.

Samples	Li	Ni	Co	Mn	Sm
Theoretical sample	1.20	0.13	0.13	0.54	0
x = 0	1.23	0.12	0.13	0.52	0
x = 0.01	1.23	0.12	0.13	0.51	0.01
x = 0.03	1.23	0.12	0.13	0.50	0.02
x = 0.05	1.23	0.12	0.13	0.49	0.03